Statistical mechanics of Roskilde liquids: Configurational adiabats, specific heat contours, and density dependence of the scaling exponent

Bailey, Nicholas; Bøhling, Lasse; Veldhorst, Arno; Schrøder, Thomas; Dyre, J. C.

Statistical mechanics of Roskilde liquids: Configurational adiabats, specific heat contours, and density dependence of the scaling exponent

Nicholas P. Bailey, Lasse Bøhling, Arno A. Veldhorst, Thomas B. Schrøder, and Jeppe C. Dyre

DNRF Center "Glass and Time," IMFUFA, Dept. of Sciences, Roskilde University, P. O. Box 260, DK-4000 Roskilde, Denmark

We derive exact results for the rate of change of thermodynamic quantities, in particular, the configurational specific heat at constant volume, C_V, along configurational adiabats (curves of constant excess entropy S_{ex}). Such curves are designated isomorphs for so-called Roskilde liquids, in view of the invariance of various structural and dynamical quantities along them. The slope of the isomorphs in a double logarithmic representation of the density-temperature phase diagram, γ, can be interpreted as one third of an effective inverse power-law potential exponent. We show that in liquids where γ increases (decreases) with density, the contours of C_V have smaller (larger) slope than configurational adiabats. We clarify also the connection between γ and the pair potential. A fluctuation formula for the slope of the C_V-contours is derived. The theoretical results are supported with data from computer simulations of two systems, the Lennard-Jones fluid, and the Girifalco fluid. The sign of $d\gamma/d\rho$ is thus a third key parameter in characterizing Roskilde liquids, after γ and the virial-potential energy correlation coefficient R. To go beyond isomorph theory we compare invariance of a dynamical quantity, the self-diffusion coefficient, along adiabats and C_V-contours, finding it more invariant along adiabats. © *2013 AIP Publishing LLC.* [http://dx.doi.org/10.1063/1.4827090]

I. INTRODUCTION

The traditional notion of a simple liquid-involving point-like particles interacting via radially symmetric pair potentials[1–13] (for example, the Lennard-Jones (LJ) system) is challenged by the existence of examples such as the Gaussian core model[14] and the Lennard-Jones Gaussian model[15,16] which exhibit complex behavior. Moreover, many molecular models have simple behavior in computer simulations, and experiments on van der Waals liquids show that these are generally regular with no anomalous behavior. We have recently suggested redefining a simple liquid—termed now a Roskilde-simple liquid, or just a Roskilde liquid—as one with strong correlations between the equilibrium virial (W) and potential-energy (U) fluctuations in the canonical fixed-volume (NVT) ensemble.[17] The basic phenomenology and theoretical understanding of Roskilde liquids were presented in a series of five papers published in the Journal of Chemical Physics.[18–22] In particular, Appendix A of Ref. 21 established an essential theorem of Roskilde liquids: A system has strong U, W correlations if and only if it has good isomorphs (curves in the thermodynamic phase diagram along which a number of properties are invariant in reduced units[21]). The degree of simplicity depends on the thermodynamic state point—all realistic systems lose simplicity when approaching the critical point and gas states. To illustrate this, Figure 1 shows the Lennard-Jones diagram including contours of the correlation coefficient R between U and W. We choose an (arbitrary) cut-off $R > 0.9$ as the boundary of simple-liquid behavior. It is clear from the figure that the correlation coefficient decreases rapidly as the liquid-gas spinodal is approached.

The theory of isomorphs starts with their definition and derives consequences from this which can be tested in simulations. For a system with N particles, two density-temperature state points (ρ_1, T_1) and (ρ_2, T_2) are isomorphic to each other if the Boltzmann factors for corresponding configurational microstates are proportional:

$$\exp\left(-\frac{U(\mathbf{r_1}^{(1)}, \ldots, \mathbf{r_N}^{(1)})}{k_B T_1}\right)$$
$$= C_{12} \exp\left(-\frac{U(\mathbf{r_1}^{(2)}, \ldots, \mathbf{r_N}^{(2)})}{k_B T_2}\right). \quad (1)$$

Here U is the potential energy function and C_{12} depends on the two state points, but not on which microstates are considered. Corresponding microstates means $\rho_1^{1/3}\mathbf{r}_i^{(1)} = \rho_2^{1/3}\mathbf{r}_i^{(2)}$, or $\tilde{\mathbf{r}}_i^{(1)} = \tilde{\mathbf{r}}_i^{(2)}$, where a tilde denotes so-called reduced units. Reduced units for lengths means multiplying by $\rho^{1/3}$, for energies dividing by $k_B T$, and for times dividing by $(m/k_B T)^{1/2}\rho^{-1/3}$ (for Newtonian dynamics). An isomorph is a curve in the phase diagram consisting of points which are isomorphic to each other. From the definition it follows that all structural and dynamical correlation functions are isomorph invariant when expressed in reduced units. Thermodynamic quantities which do not involve volume derivatives, such as the excess entropy S_{ex} and excess specific heat at constant volume C_V^{ex}, are also isomorph invariant. Another consequence of the isomorph definition is that phase boundaries lying within the simple region of the phase diagram are isomorphs—note that the isomorph shown in Fig. 1 is nearly parallel to the liquid-solid coexistence lines. Reference 28
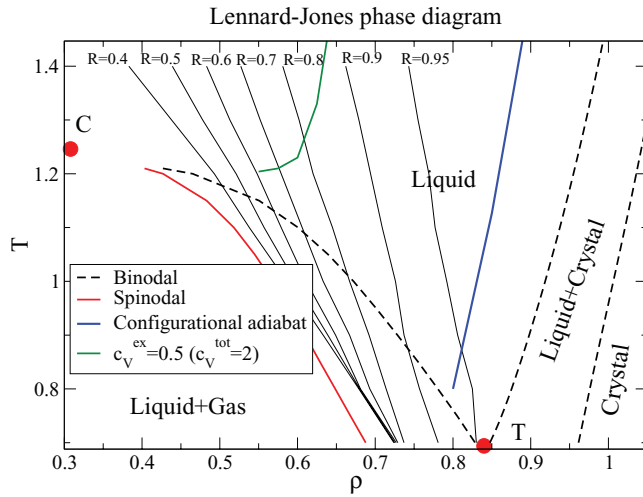
FIG. 1. Contour plot of R in (ρ, T) phase diagram for the single-component Lennard-Jones system using a shifted-potential cutoff of 4σ and system size $N = 1000$. Contour values are indicated at the top. Also indicated are binodal and spinodal obtained from the Johnson equation of state with the cutoff taken into account in a mean-field manner,[23] and the corresponding curves for solid-liquid coexistence as parameterized by Mastny and de Pablo (though for the larger cutoff 6σ).[24] T and C indicate the triple[24] and critical[23] points. The blue curve is a configurational adiabat, while the green line is the configurational isochoric specific heat contour $C_V = Nk_B/2$ (total specific heat $2Nk_B$); this is one of the criteria for the dynamic crossover separating liquid and gas regions in the phase diagram proposed by Brazhkin *et al.*[25–27] According to the theory of isomorphs both configurational adiabats and C_V-contours are isomorphs for sufficiently large R (Eq. (2)).

gives a brief review of the theory and its experimentally relevant consequences.

Only inverse power-law (IPL) systems, i.e., systems for which the potential energy is an Euler homogeneous function, have 100% virial potential-energy correlation and perfect isomorphs. Thus for realistic Roskilde liquids the isomorph concept is only approximate. Extensive computer simulations have shown, however, that the predicted isomorph invariants apply to a good approximation for several systems.[17, 21, 22, 29–33] A few predictions have also been confirmed experimentally.[33, 34]

Despite the success of the isomorph concept, it remains a "zero-order" theory, analogous to the ideal gas. In particular, there is no systematic theory for describing realistic systems in terms of perturbations about the ideal case. The purpose of this work is to examine deviations from perfect isomorph behavior in Roskilde liquids. One motivation is to understand what kind of deviations from IPL behavior (for example, constancy of the scaling exponent) are allowed while remaining in the "simple part" of the phase diagram. A second motivation is the hope of using Roskilde liquids to identify a general theory of liquids. For example, the existence of good isomorphs explains many observed connections between dynamics, structure, and thermodynamics, but also means that cause-and-effect interpretations of such connections ("the dynamics is *controlled* by ...") must be reexamined. Given perfect isomorphs, any isomorph-invariant quantity can be said to control all the others. This puts a constraint on general theories, referred to as the "isomorph filter,"[21] but prevents one from sorting among theories that pass the filter. Examin-

ing carefully whether dynamical properties are more invariant when holding one isomorph-invariant quantity fixed versus holding another fixed could provide a means to select theories. The above applies equally well to theories of supercooled liquids and the glass transition; for example, in a theory featuring a characteristic activation energy or a characteristic temperature such as the Kauzmann temperature, then requiring the theory to pass the isomorph filter means that the characteristic energy/temperature depends on density in a specific manner.

Strong U, W correlation in the equilibrium NVT ensemble is a hallmark, and the first identified feature,[35] of Roskilde liquids. It is characterized at the level of second moments by the correlation coefficient

$$R(\rho, T) = \frac{\langle \Delta U \Delta W \rangle}{\sqrt{\langle (\Delta U)^2 \rangle \langle (\Delta U)^2 \rangle}} \qquad (2)$$

and the slope

$$\gamma(\rho, T) = \frac{\langle \Delta U \Delta W \rangle}{\langle (\Delta U)^2 \rangle}. \qquad (3)$$

Here Δ represents the deviation of a quantity from its NVT ensemble average. It has been shown that γ may be thought of in terms of an effective IPL potential with exponent 3γ (which in general depends on state point).[18, 19] It has also a thermodynamic interpretation, namely, it is the ratio of the excess pressure coefficient $\beta_V^{ex} \equiv (1/V)(\partial W/\partial T)_V$ and excess specific heat per unit volume,

$$\gamma = \frac{\beta_V^{ex}}{c_V^{ex}}. \qquad (4)$$

As mentioned, in IPL systems the correlation is indeed perfect, but non-IPL systems exist which yet have strong U, W-correlations, in particular the usual LJ fluid. While in any system the fluctuation formula for γ can be used to generate curves of constant (excess) entropy S_{ex} (configurational adiabats) via[21]

$$\left(\frac{\partial \ln T}{\partial \ln \rho} \right)_{S_{ex}} = \gamma(\rho, T), \qquad (5)$$

in Roskilde-simple liquids several properties related to structure, thermodynamics, and dynamics are invariant along these curves. This leads to their designation as "isomorphs"; note that quantities must be expressed in thermodynamically reduced units to exhibit the invariance.[21] As an example of a structural quantity, the radial distribution function $g(r)$ is typically found to collapse well when plotted in reduced units along an isomorph; it could be that higher order measures of structure are less invariant, though.[36] One of the most basic isomorph-invariant quantities is the specific heat at constant volume: perfect isomorphs are also C_V-contours, while in imperfectly correlating systems the C_V contours and configurational adiabats may differ.

One might expect that the closer R is to unity, the better approximated the system would be by a single IPL potential. So it is perhaps surprising that we have recently identified systems where γ changes much more than in the LJ case, over a range in which strong U, W-correlation ($R > 0.9$) is maintained. One such system is the "repulsive Lennard-Jones" potential, in which the sign of the $1/r^6$ term is made positive.[32] It

seems that the property of strong U, W correlation and the existence of isomorphs are somehow more robust than the constancy of γ. It can be surprising how well isomorphs "work" for non-IPL systems. This robustness allows for a richer variety of behavior, since the shapes of isomorphs are no longer necessarily straight lines in a $(\ln \rho, \ln T)$-plot. The theory of the thermodynamics of Roskilde-simple liquids[32] implies that γ may be considered a function of ρ only. This immediately gives us a new quantity (in addition to R and γ) to characterize Roskilde liquids: $d\gamma/d\rho$, or more simply, its sign. This result depends on the assumption that configurational adiabats and C_V-contours exactly coincide. It is not clear what to expect when this does not hold exactly; this paper is an attempt to address the topic of imperfect correlation from statistical mechanical considerations. Because C_V is also a fundamental thermodynamic quantity, the difference between adiabats and C_V-contours should be a useful probe of the breakdown of perfect isomorphs as U, W-correlation becomes less than perfect, and will be the focus of this paper.

While, as mentioned above, the arguments of Ref. 32 (which assume perfect isomorphs) show that $\gamma = \gamma(\rho)$, in practice γ does depend on T but the dependence is much smaller than that on ρ, and we can ignore it most of the time. This is apparent for the single-component LJ system in Fig. 5 of Ref. 18. A more explicit quantitative comparison, of the logarithmic derivatives of γ with respect to ρ and T, was made in Ref. 33 for two molecular systems. We present further data on this below. Fluids with LJ and similar potentials (for example, generalized-LJ potentials with different exponents) tend to have $d\gamma/d\rho < 0$: It is clear that γ must converge to one third of the repulsive exponent at very high densities and temperatures while typical values are larger.[19] On the other hand, potentials may be constructed which have $d\gamma/d\rho > 0$, simply by shifting the potential radially outwards so that the repulsive divergence occurs at a finite value of pair separation. Such potentials naturally involve a hard core of absolutely excluded volume. They are relevant to experiments,[33] because tests of the isomorph theory[34] typically involve molecules rather than single atoms, with the interaction range being relatively short compared to the particle size (colloids are an even more extreme example of this, of course). The Dzugutov system,[37] although only Roskilde-simple at high densities and temperatures, is another example with $d\gamma/d\rho > 0$, but where there is no hard core. Another such system is the above-mentioned repulsive Lennard-Jones potential; in this case the effective exponent increases monotonically, interpolating between the low density limit 6 ($\gamma = 2$) and the high density limit 12 ($\gamma = 4$).

For brevity we term curves of constant S_{ex} *adiabats* (the qualifier "configurational" is to be understood); in this paper, unlike all our other works on isomorphs, we deliberately avoid calling them isomorphs, since the point of this work is to examine deviations from perfect isomorph behavior. We also drop the subscript ex for notational simplicity, and similarly use C_V to mean the configurational part of specific heat (the kinetic part is also isomorph invariant, though, being 3/2 for a classical monatomic system). Below we derive some exact results concerning the relation between adiabats and C_V-

contours, and argue how this connects to whether γ is an increasing or decreasing function of ρ (more specifically the sign of $(\partial\gamma/\partial\rho)_S$). The argument involves relating γ to an exponent determined by derivatives of the pair potential, introduced in Ref. 19. The claim is supported by simulations of two Roskilde liquids: the LJ fluid (with $d\gamma/d\rho < 0$) and the Girifalco fluid (with $d\gamma/d\rho > 0$ at least for high densities). The Girifalco potential was constructed to model the effective interaction between C_{60} molecules, modeling the carbon atoms as Lennard-Jones particles and applying rotational averaging:[38]

$$v(r) = -\alpha\left(\frac{1}{s(s-1)^3} + \frac{1}{s(s+1)^3} - \frac{2}{s^4}\right)$$
$$+\beta\left(\frac{1}{s(s-1)^9} + \frac{1}{s(s+1)^9} - \frac{2}{s^{10}}\right). \quad (6)$$

where s is the distance two molecules' centers, scaled by the diameter. We have chosen the parameters α and β such that the potential well has a depth of approximately 1 and the potential diverges at unit distance, $\beta = 0.0018141\alpha$ with $\alpha = 0.17$.

For simulations we use systems of 1000 particles simulated at constant volume and temperature (NVT) using the RUMD code[39] for simulating on NVIDIA graphical processing units (GPUs). Although the state points considered do not involve long relaxation times, the speed provided by GPUs is desirable because reasonably accurate determination of third moments requires of order 1×10^6 independent samples; we typically run 50×10^6 steps and sample every 50 steps (the time step sizes were 0.0025–0.004 for LJ and 0.0004 for Girifalco). The temperature was controlled using a Nosé-Hoover thermostat. Part (d) in Fig. 3 shows the correlation coefficient R along an adiabat for each system. Both systems are Roskilde-simple (have $R > 0.9$) in the simulated part of the phase diagram.

In Sec. II, a general fluctuation formula for derivatives of thermodynamic quantities along adiabats is derived, and applied to the case of C_V. In Sec. III we show the connection between the derivative of C_V and derivatives of γ. The results are illustrated with data from simulations. In Sec. IV a fluctuation formula for the slope of contours of C_V is derived, and illustrated with simulation data. Finally, Secs. V and VI are the discussion and a brief conclusion, respectively.

II. THERMODYNAMIC DERIVATIVES AT CONSTANT ENTROPY

A. γ as linear-regression slope

Before proceeding to thermodynamic derivatives we recall the connection between the above definition of γ and linear regression. Following Appendix C of Ref. 21 we characterize the deviation from perfect correlation via the fluctuating variable

$$\epsilon \equiv \Delta W - \gamma \Delta U, \quad (7)$$

which vanishes for perfect correlation. The linear regression slope is defined by minimizing $\langle\epsilon^2\rangle$ with respect to γ, leading to Eq. (3).[40] A consequence of this definition of γ is seen by

writing

$$\Delta W = \gamma \Delta U + \epsilon, \tag{8}$$

and correlating[41] this with ΔU:

$$\langle \Delta W \Delta U \rangle = \gamma \langle (\Delta U)^2 \rangle + \langle \Delta U \epsilon \rangle \tag{9}$$

From this and the definition of γ it follows that

$$\langle \Delta U \epsilon \rangle = 0, \tag{10}$$

that is, U and ϵ are (linearly) uncorrelated, independent of whether perfect correlation holds between U and W.

B. Density-derivatives of averages on adiabats

We are interested in the derivatives of thermodynamic quantities along certain curves in the phase diagram, in particular those of constant S, so we start by presenting general formulas for the derivatives with respect to $\ln \rho$ and $\ln T$ (holding the other constant). From standard statistical mechanics (see, for example, Appendix B of Ref. 18) we have (with $\beta = 1/(k_B T)$; in the following we set $k_B = 1$)

$$\left(\frac{\partial \langle A \rangle}{\partial \beta} \right)_\rho = - \langle \Delta U \Delta A \rangle \tag{11}$$

which implies

$$\left(\frac{\partial \langle A \rangle}{\partial \ln T} \right)_\rho = \beta \langle \Delta U \Delta A \rangle. \tag{12}$$

Likewise (see Appendix A),

$$\left(\frac{\partial \langle A \rangle}{\partial \ln \rho} \right)_T = \left\langle \frac{\partial A}{\partial \ln \rho} \right\rangle - \beta \langle \Delta W \Delta A \rangle, \tag{13}$$

where differentiation with respect to $\ln \rho$ inside an expectation value—that is, for an arbitrary configuration rather than an ensemble average—is understood to imply that the reduced coordinates of the configuration, $\tilde{\mathbf{r}}_i \equiv \rho^{1/3} \mathbf{r}_i$, are held fixed. Equations (12) and (13) can be used to construct the derivative with respect to $\ln \rho$ along an arbitrary direction; that is instead of keeping T constant (a line of zero slope) we take a direction with slope g (in $\ln \rho$, $\ln T$ space):

$$\left(\frac{\partial \langle A \rangle}{\partial \ln \rho} \right)_{[g]} = \left(\frac{\partial \langle A \rangle}{\partial \ln \rho} \right)_T + g \left(\frac{\partial \langle A \rangle}{\partial \ln T} \right)_\rho \tag{14}$$

$$= \left\langle \frac{\partial A}{\partial \ln \rho} \right\rangle - \beta \langle \Delta W \Delta A \rangle + g \beta \langle \Delta U \Delta A \rangle \tag{15}$$

$$= \left\langle \frac{\partial A}{\partial \ln \rho} \right\rangle - \beta \langle \Delta A (\Delta W - g \Delta U) \rangle. \tag{16}$$

Note that we use subscript $[g]$ to indicate that g is the slope in the $\ln \rho$, $\ln T$ plane, rather than the quantity held constant, in the derivative. This expression can be used to find formulas for the direction in which a given thermodynamic variable is constant, as we do below. For now we choose $g = \gamma$, to obtain

a formula for derivatives along adiabats (Eq. (5)):

$$\left(\frac{\partial \langle A \rangle}{\partial \ln \rho} \right)_S = \left\langle \frac{\partial A}{\partial \ln \rho} \right\rangle - \beta \langle \Delta A \Delta (W - \gamma U) \rangle$$

$$= \left\langle \frac{\partial A}{\partial \ln \rho} \right\rangle - \beta \langle \Delta A \epsilon \rangle. \tag{17}$$

As an example, we take $A = U$. Noting that $W \equiv \partial U / \partial \ln \rho$ and Eq. (10), we get

$$\left(\frac{\partial \langle U \rangle}{\partial \ln \rho} \right)_S = \left\langle \frac{\partial U}{\partial \ln \rho} \right\rangle = \langle W \rangle, \tag{18}$$

which is a general result that can also be derived thermodynamically starting with the fundamental thermodynamic identity $T dS = dU + p dV = dU + W d \ln(V) = dU - W d \ln \rho$ (here the variables U, W refer to macroscopic, or thermally averaged quantities, the omission of angle-brackets notwithstanding). As a second application of Eq. (17), consider a system with perfect correlation. Then $\epsilon \equiv 0$, and we get

$$\left(\frac{\partial \langle A \rangle}{\partial \ln \rho} \right)_S = \left\langle \frac{\partial A}{\partial \ln \rho} \right\rangle, \tag{19}$$

which means that in such systems the derivative along an adiabat is given entirely by the "intrinsic" density dependence for individual configurations; fluctuations do not contribute. This is of course the case of perfect isomorphs, where the probabilities of scaled configurations are identical along an isomorph.

C. Variation of C_V on adiabats

We consider the derivative of C_V with respect to $\ln \rho$ on an adiabat. From $C_V = \langle (\Delta U)^2 \rangle / T^2$, we have

$$\left(\frac{\partial C_V}{\partial \ln \rho} \right)_S = \frac{1}{T^2} \left(\frac{\partial \langle (\Delta U)^2 \rangle}{\partial \ln \rho} \right)_S - \frac{2}{T^3} \langle (\Delta U)^2 \rangle \left(\frac{\partial T}{\partial \ln \rho} \right)_S \tag{20}$$

$$= \frac{1}{T^2} \left(\frac{\partial \langle (\Delta U)^2 \rangle}{\partial \ln \rho} \right)_S - \frac{2\gamma}{T^2} \langle (\Delta U)^2 \rangle. \tag{21}$$

Writing $\langle (\Delta U)^2 \rangle = \langle U^2 \rangle - \langle U \rangle^2$ and making use of the general result of Eq. (17), after some algebra (see Appendix B) we obtain the simple result

$$\left(\frac{\partial C_V}{\partial \ln \rho} \right)_S = -\beta^3 \langle (\Delta U)^2 \Delta (W - \gamma U) \rangle = -\beta^3 \langle (\Delta U)^2 \epsilon \rangle. \tag{22}$$

This is a major result of this paper. Note that the right side vanishes for perfect correlation ($\epsilon = 0$)—in which case C_V is constant on the same curves that S is; in other words, C_V is a function of entropy only. For less than perfect correlation, the most interesting feature is the sign, which we argue in Sec. III, is the opposite of that of $d\gamma/d\rho$.

III. CONNECTION BETWEEN $(\partial C_V/\partial\rho)_S$ AND DERIVATIVES OF γ

A. Relation to temperature-dependence of γ

We wish to understand the sign of $\langle(\Delta U)^2\epsilon\rangle$. We know from Eq. (10) that U and ϵ are linearly uncorrelated; we must now consider higher order correlations. Recall that γ may also be interpreted[18] as the slope of isochores in the W, U phase diagram—the linear regression of the scatter-plot of instantaneous W, U values at one state point gives the slope of $\langle W\rangle$ versus $\langle U\rangle$ at fixed density. The triple correlation is related to the curvature of the isochore, and thus to $(\partial\gamma/\partial T)_\rho$. We obtain the exact relation by differentiating γ with respect to β:

$$\left(\frac{\partial\gamma}{\partial\beta}\right)_\rho = \frac{1}{\langle(\Delta U)^2\rangle}\left(\frac{\partial\langle\Delta U\Delta W\rangle}{\partial\beta}\right)_\rho$$
$$-\frac{\langle\Delta U\Delta W\rangle}{\langle(\Delta U)^2\rangle^2}\left(\frac{\partial\langle(\Delta U)^2\rangle}{\partial\beta}\right)_\rho \quad (23)$$

$$= -\frac{\langle(\Delta U)^2\Delta W\rangle}{\langle(\Delta U)^2\rangle} - \frac{\gamma}{\langle(\Delta U)^2\rangle}\left(-\langle(\Delta U)^3\rangle\right) \quad (24)$$

$$= -\frac{\langle(\Delta U)^2(\Delta W - \gamma\Delta U)\rangle}{\langle(\Delta U)^2\rangle} \quad (25)$$

$$= -\frac{\langle(\Delta U)^2\epsilon\rangle}{\langle(\Delta U)^2\rangle}, \quad (26)$$

where we have used Eq. (11) and some algebraic manipulation as in Appendix B. Combining this result with Eq. (22) gives

$$\left(\frac{\partial C_V}{\partial\ln\rho}\right)_S = \beta^2\langle(\Delta U)^2\rangle\beta\left(\frac{\partial\gamma}{\partial\beta}\right)_\rho = -C_V\left(\frac{\partial\gamma}{\partial\ln T}\right)_\rho, \quad (27)$$

or more concisely

$$\left(\frac{\partial\ln C_V}{\partial\ln\rho}\right)_S = -\left(\frac{\partial\gamma}{\partial\ln T}\right)_\rho. \quad (28)$$

B. Relation to density-dependence of γ via the effective IPL exponent $n^{(2)}(r)$

The last result implies, in particular, that the sign of the density-derivative of C_V along an isomorph is opposite to that of $(\partial\gamma/\partial T)_\rho$. Since the latter derivative is neglected in the theory of isomorphs, it is useful to find a connection with a density derivative of γ. The relevant derivative turns out not to be $(\partial\gamma/\partial\rho)_T$ but $(\partial\gamma/\partial\rho)_S$, i.e., the derivative of γ along the adiabat. For many systems of interest this derivative has the same sign as $(\partial\gamma/\partial T)_\rho$, while those signs can be positive or negative depending on the system (or even for a given system). We shall now argue that this sign-equivalence is to be expected by considering how γ is related to the pair potential $v(r)$. This is an interesting question in its own right, and was explored in Ref. 19. For potentials with strong repulsion at short distances, we can indeed relate γ directly, albeit approximately, to $v(r)$, or more precisely, to its derivatives. As

discussed in Ref. 19 the idea is to match an IPL to the actual potential; γ is then one third of the "effective IPL exponent." There are many ways to define such an exponent, but a key insight is that it should involve neither the potential itself (because shifting the zero of potential has no consequences), nor its first derivative (because the contributions to the forces from a linear term tend to cancel out in dense systems at fixed volume).[19] The simplest possibility within these constraints involves the ratio of the second and third derivatives. For an IPL, $v(r) \propto 1/r^n$, and indicating derivatives with primes, we have $v'''(r)/v''(r) = -(n+2)/r$, so n can be extracted as $-rv'''(r)/v''(r) - 2$. For a general pair potential this quantity will be a function of r, and thus we define the r-dependent second-order effective IPL exponent $n^{(2)}(r)$ as[19]

$$n^{(2)}(r) \equiv -\frac{rv'''(r)}{v''(r)} - 2. \quad (29)$$

The superscript "(2)" indicates which derivative appears in the denominator; one can similarly[19] define $n^{(p)}(r)$ for $p = 0, 1, \ldots$; $p = 2$ is the first not involving v or v'. Interestingly, the IPL is not the only solution to $n^{(2)}(r) = n$ with constant n; so is the so-called extended IPL

$$v_{\text{eIPL}}(r) = A/r^n + Br + C, \quad (30)$$

introduced in Ref. 19. The resemblance of the Lennard-Jones potential to such a form can be considered an explanation of why it inherits many of the properties of the IPL potential. For a general potential, the question that now arises is at which r one should evaluate $n^{(2)}$. It was argued in Ref. 19 that $n^{(2)}/3$ evaluated at a point near the maximum of $g(r)$—let us call it r_γ—should correspond to γ. One expects that, like the peak in $g(r)$, $r_\gamma = \Lambda\rho^{-1/3}$, where Λ is of order unity and depends weakly on temperature, but we do not know it precisely *a priori*. There are two crucial things we can say, however: First, we can certainly identify r_γ *a posteriori* by inspection for a given state point: That is, having simulated a reference state point $(\rho_{\text{ref}}, T_{\text{ref}})$ and determined γ_{ref} there, it is straightforward to (typically numerically) solve the equation $n^{(2)}(r_\gamma)/3 = \gamma_{\text{ref}}$ for r_γ. The second crucial point is that whatever details of the liquid's statistical mechanics determine r_γ (for instance, a kind of $g(r)$-weighted average), *these details do not vary along an isomorph* (this argument assumes good isomorphs, so that the statement can be applied to adiabats). Therefore, r_γ is an isomorph invariant—more precisely its reduced-unit form $\rho^{1/3}r_\gamma = \Lambda$ is constant along an adiabat, which implies $\Lambda = \Lambda(S)$. So γ is given by

$$\gamma(\rho, S) = \frac{1}{3}n^{(2)}(\Lambda(S)\rho^{-1/3}), \quad (31)$$

or

$$\gamma(\rho, S) = \frac{1}{3}n^{(2)}\left(r_{\gamma,\text{ref}}(S)\frac{\rho^{-1/3}}{\rho_{\text{ref}}^{-1/3}}\right). \quad (32)$$

In the form with Λ we explicitly recognize that Λ is constant on an isomorph, or equivalently, that it depends on S; the second form shows how Λ can be determined using a simulation at one density to identify r_γ there.

For the Lennard-Jones potential $n^{(2)}(r)$ decreases as r decreases (corresponding to as ρ increases), while for potentials such as the Girifalco potential with a divergence at finite r (see Fig. 3), it increases as r decreases (ρ increases), although at low densities the opposite behavior is seen. The validity of Eq. (31) has been investigated by Bøhling *et al.*[42] Under which circumstances does Eq. (31) give a good estimate of the density dependence of γ? The system must have sufficiently strong W, U correlations, since as $R \to 0$, γ must also vanish irrespective of $n^{(2)}$'s behavior. (For example, in a Lennard-Jones-like liquid, as r increases, the curvature of the pair potential becomes negative at some r, at which point $n^{(2)}$ diverges. At or below the corresponding density, and not too high temperature, a single phase is likely to have a negative pressure and be mechanically unstable, giving way to liquid-gas coexistence. In this regime W, U correlations tend to break down completely and γ goes to zero; see Figs. 3(c) and 3(d), in particular the Girifalco data.)

Equation (31) shows how γ depends on ρ, but we need to consider temperature dependence in order to connect with the result for C_V along an adiabat. This comes in through $\Lambda(S)$. We cannot right away determine how Λ depends on S but we know it is a weak dependence, since r_γ is expected to remain close to the peak in $g(r)$.[42] For liquids with a repulsive core this peak moves slowly to shorter distances as temperature, and hence entropy, increase at fixed ρ. We expect the same to be true for Λ, since in the high-temperature limit potential energy and virial fluctuations, and thus γ, are dominated by ever smaller pair separations. Thus we expect that

$$\frac{d\Lambda(S)}{dS} < 0, \tag{33}$$

while the weak dependence on entropy/temperature at fixed density can be expressed as

$$C_V \frac{d\ln\Lambda(S)}{dS} \ll 1, \tag{34}$$

(the use of C_V to make the left side dimensionless, instead of, for example, differentiating with respect to $\ln S$, is done for convenience below; note that C_V varies slowly and has a similar order of magnitude to the entropy differences between isomorphs in the liquid region of the phase diagram). From Eq. (33) it follows that both increasing ρ at fixed S, and increasing T at fixed ρ, decrease the argument of $n^{(2)}$. (Recall that in the earliest work on Roskilde liquids it was noted that the slope of the W, U correlation converges down towards $12/3 = 4$ for the LJ case both in the high temperature and the high density limits.[35]) Taking the appropriate derivatives of Eq. (31) yields

$$\left(\frac{\partial\gamma}{\partial\ln\rho}\right)_S = -\frac{\Lambda(S)\rho^{-1/3}}{9}\left.\frac{dn^{(2)}(r)}{dr}\right|_{r=\Lambda(S)\rho^{-1/3}}, \tag{35}$$

$$\left(\frac{\partial\gamma}{\partial\ln T}\right)_\rho = \frac{\Lambda(S)\rho^{-1/3}}{3}\left.\frac{dn^{(2)}(r)}{dr}\right|_{r=\Lambda(S)\rho^{-1/3}}\frac{d\ln(\Lambda(S))}{dS}C_V. \tag{36}$$

TABLE I. Validity of Eq. (38) for several potentials. For each system the signs of $(\partial\gamma/\partial T)_\rho$ and $(\partial\gamma/\partial\rho)_S$ have been checked for a set of adiabats. For the Lennard-Jones, Buckingham and Dzugutov system the density range gives the lowest densities of the simulated adiabats while the temperature range gives the range of temperatures simulated for each adiabat. For the Girifalco and repulsive Lennard-Jones the density range indicates the range of densities simulated for each adiabat, while the temperature range indicates the lowest temperatures. Data near extrema of γ have not been included.

Potential	ρ-range	T-range	$(\partial\gamma/\partial T)_\rho$	$(\partial\gamma/\partial\rho)_S$
Lennard-Jones	0.6–1.2	0.8–5.0	−	−
Buckingham	0.7–1.2	2–6	−	−
Dzugutov	0.55–0.8	0.75–1.2	+	+
Girifalco	0.45–0.5	6–54	+	+
Repulsive Lennard-Jones	0.1–10	0.4–2.0	+	+

Combining these gives

$$\left(\frac{\partial\gamma}{\partial\ln T}\right)_\rho = \left(\frac{\partial\gamma}{\partial\ln\rho}\right)_S\left(-3\frac{d\ln(\Lambda(S))}{dS}C_V\right). \tag{37}$$

From Eqs. (33) and (34) the quantity in brackets on the right side is positive but much smaller than unity. We therefore have

$$\mathrm{sgn}\left(\left(\frac{\partial\gamma}{\partial T}\right)_\rho\right) = \mathrm{sgn}\left(\left(\frac{\partial\gamma}{\partial\rho}\right)_S\right),$$
$$\left|\left(\frac{\partial\gamma}{\partial\ln T}\right)_\rho\right| \ll \left|\left(\frac{\partial\gamma}{\partial\ln\rho}\right)_S\right|, \tag{38}$$

which is expected to hold for liquids with repulsive cores, with sufficiently strong W, U-correlations. It remains to be investigated thoroughly to what extent Eq. (38) holds, both regarding in how large a region of the phase diagram it holds for a given liquid, and for which liquids it holds in a reasonably large region. Its validity depends both on that of Eq. (31) and the conjecture that Λ decreases, slowly, as entropy increases. Some data are shown in Table I which compares the signs of the two derivatives for different systems and Fig. 2 which compares the two derivatives at state points along an adiabat for the LJ system. For comparison the density derivative at fixed temperature is also shown, obtained via chain-rule combination of the other two derivatives. This involves a minus sign and therefore the two terms (which have the same sign) tend to cancel.

In the limit of perfect W, U correlation we know $(\partial\gamma/\partial T)_\rho$ vanishes. There is no reason to expect Λ to become constant in this limit,[43] therefore $(\partial\gamma/\partial\rho)_S$ must also vanish in the limit. This corresponds to $n^{(2)}(r)$ becoming constant: IPL or extended IPL systems (Eq. (30)). But because the dependence of Λ on S is in general weak, there is a regime—that of general Roskilde liquids—where we can neglect it, but where $n^{(2)}$ cannot be considered constant. In this approximation, then, we can write the density derivative as an ordinary derivative. Combining this with Eq. (28) we have the following result for the sign of the C_V:

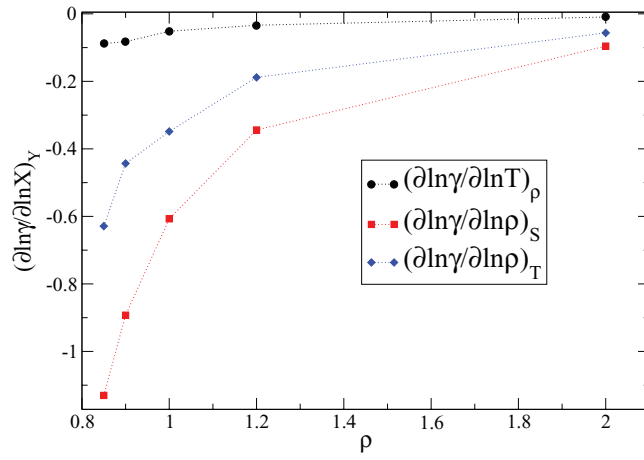$$\mathrm{sgn}\left(\left(\frac{\partial C_V}{\partial\ln\rho}\right)_S\right) = -\mathrm{sgn}\left(d\gamma/d\rho\right). \tag{39}$$

FIG. 2. Logarithmic derivatives of γ: (1) with respect to T at constant ρ, (2) respect to ρ at constant S and (3) respect to ρ at constant T, for the LJ system at points along the adiabat including $\rho = 0.85$, $T = 0.80$. The first derivative was determined via fitting $\ln(\gamma)$ versus $\ln T$ data (obtained also for neighboring adiabats) at each ρ to a quadratic function; the second analytically after making a (one-parameter) fit to the logarithmic derivative of Eq. (C5); and the third via the chain rule as a linear combination of the other two, $(\partial \ln(\gamma)/\partial \ln \rho)_T = (\partial \ln(\gamma)/\partial \ln \rho)_S - \gamma(\partial \ln(\gamma)/\partial \ln T)_\rho$. While all decrease to zero at high densities (consistent with γ converging to a constant 4 = 12/3) the temperature derivative is consistently a factor of ten smaller than the density derivative at constant S.

Thus, we can predict—based on the $n^{(2)}$ estimate of γ—that the rate of change of C_V along an adiabat has the opposite sign as the density dependence of γ (along the adiabat if we need to be specific). Thus from knowing only the pair potential one can say something reasonably accurate about both the adiabats and the C_V-contours.

C. Simulation results for variation of C_V along adiabats

To confirm the relation between the sign of $d\gamma/d\rho$ and that of $(\partial C_V/\partial \rho)_S$ and exhibit the relation between adiabats and C_V contours we carried out simulations on two model systems. Figure 3(a) shows the pair potentials. Note that the Girifalco potential diverges at $r = 1$; this hard core restricts the density to be somewhat smaller than for the LJ case. Part (b) of Fig. 3 shows the effective exponent $n^{(2)}(r)$. There is a singularity where the second derivative vanishes (the transition from concave up to concave down), which can be seen in the figure at $r \simeq 1.224$ for LJ and $r \simeq 1.48$ for Girifalco; as r decreases from the singularity $n^{(2)}$ decreases monotonically in the LJ case, while in the Girifalco case it first decreases and then has a minimum before increasing and in fact diverging as $r = 1$ is approached. Part (c) of Fig. 3 shows the estimate of $\gamma(\rho)$ from Eq. (31) along with $\gamma(\rho)$ calculated in simulations along an adiabat for each system. Here Λ was determined by matching $n^{(2)}/3$ with γ at the highest density. The agreement is good for not too low densities—as mentioned above when $n^{(2)}(r)$ diverges due to the curvature of the potential vanishing, then both R and γ will rapidly approach zero, which is what we can see happening for the Girifalco system in parts (c) and (d) and low density. Note that the adiabat for the Girifalco system rapidly reaches rather high temperatures, since the ex-
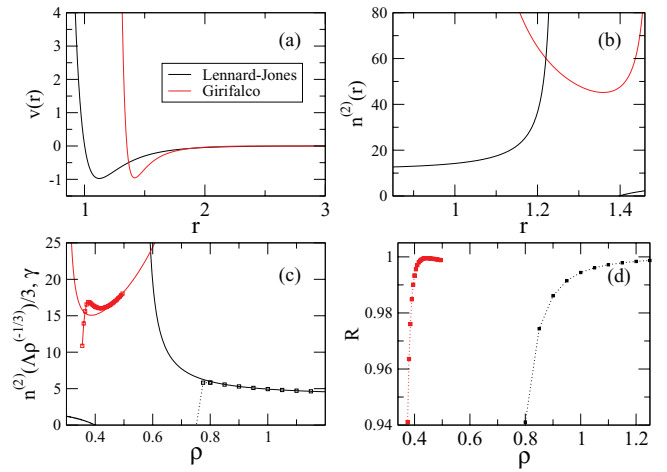

FIG. 3. (a) The pair potentials used in this work. The Girifalco potential diverges at $r = 1$. (b) $n^{(2)}(r)$ for the two potentials. (c) $n^{(2)}(\Lambda\rho^{-1/3})$ (full lines) and γ on sample adiabats for both models (symbols). The entropy was not calculated, but adiabats are uniquely specified by giving one state point, for example, $\rho = 0.80$, $T = 0.80$ for the LJ case and $\rho = 0.4$, $T = 4.0$ for the GF case. The value of Λ was fixed by requiring agreement with γ at the highest simulated density for each isomorph. (d) Correlation coefficient R from simulations, along the same adiabats as in (c).

ponent is always greater than 15, or roughly three times that of the LJ system. More interestingly, for the Girifalco system $d\gamma/d\rho$ changes sign at a density around 0.4, so we can expect the dependence of C_V along an adiabat to reflect this. The location and value of the minimum in γ do not match those for $n^{(2)}$, however—perhaps the vanishing of the curvature is already having an effect.

The procedure for determining adiabats is described in Appendix C. Figures 4 and 5 show $c_V = C_V/N$ along adiabats for the LJ and Girifalco systems, respectively. For the LJ case the slope is positive, which is consistent with $d\gamma/d\rho$ being negative as discussed in Sec. III. It is worth noting that the overall variation of C_V is quite small, of order 0.1 per particle for the density range shown, but it is not negligible,
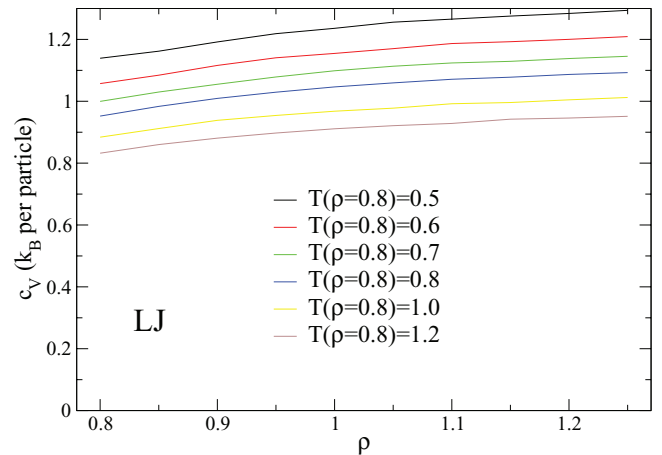

FIG. 4. Dependence of $c_V = C_V/N$ on density along six different adiabats for the LJ fluid. We label the curves by their temperature at a fixed density, here the starting density $\rho = 0.8$. The change in c_V is of order 0.1–0.15 for the ~50% change in density shown here, small but not negligible. The slopes are positive, consistent with the negative sign of $d\gamma/d\rho$ and arguments of Sec. III.
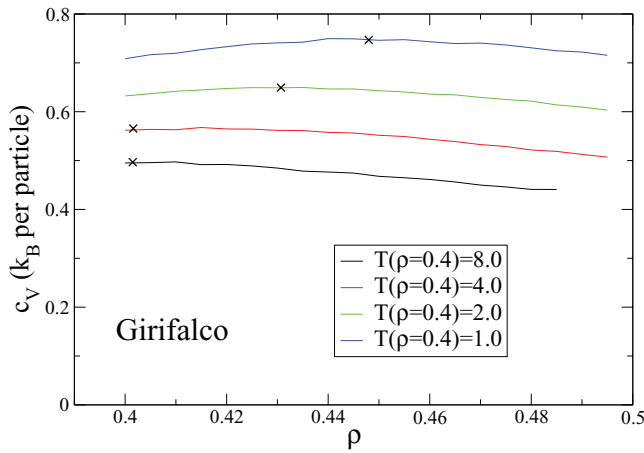
FIG. 5. Dependence of $c_V = C_V/N$ on density along four different adiabats for the Girifalco fluid. The curves are labelled by their temperature at $\rho = 0.4$. For the $\sim 20\%$ changes in density shown here, c_V changes by about 0.05. It is generally decreasing in the range shown but increases at low densities and temperatures; the maxima (determined by fitting a cubic polynomial) are shown as crosses, and appear at different densities for different adiabats.

FIG. 6. Comparison of adiabats and C_V-contours for the LJ system. The adiabats are the same as those shown in Fig. 4, and were calculated using Eq. (C3), while C_V-contours (values 0.9, 1.0, 1.1, and 1.2 in units of k_B) were determined from a series of simulations on different isochores and interpolating the C_V data as a function of T (some extrapolated points, indicated, were also included).

even though the system has strong U, W correlations and the structure and dynamics have been shown to be quite invariant along the adiabats. For the Girifalco system the slope is positive at low density until a maximum is reached, with a negative slope at higher densities. This is also broadly consistent with the expectations from Fig. 3 (the locations of the maxima are not expected to be accurately given by Eq. (31)).

D. Contours of C_V and S directly compared

As an alternative to considering how C_V varies along an adiabat, we can find the contours of C_V separately. First we simulated several isochores, then the data were interpolated to allow constant-C_V curves to be constructed. Specifically, we find that the dependence of C_V on temperature along an isochore can be accurately fitted by the expression

$$C_V(T) = \frac{A(\rho)}{T^{B(\rho)}} + C(\rho), \qquad (40)$$

where A, B, and C are functions of ρ. This expression was inspired by the Rosenfeld-Tarazona expression $C_V \sim T^{-2/5}$ for the specific heat;[44] we do not constrain the exponent B to be 2/5, however. The expression can easily be inverted to yield the temperature $T_{C_V}(\rho)$ corresponding to a given value of C_V, as a function of density

$$T_{C_V}(\rho) = \left(\frac{A(\rho)}{C_V - C(\rho)} \right)^{1/B(\rho)}. \qquad (41)$$

The C_V contours are shown along with the adiabats in Figs. 6 and 7. Recall that in typical liquids we expect C_V to increase as T decreases or ρ increases. For the LJ case the C_V contours have a higher slope than the adiabats, therefore as ρ increases along an adiabat we cross contours corresponding to higher values of C_V. For the Girifalco system the C_V contours have initially (at low density) higher slopes than the adiabats but then bend over and have lower slopes. Thus the picture is consistent with the data for C_V along adiabats shown in
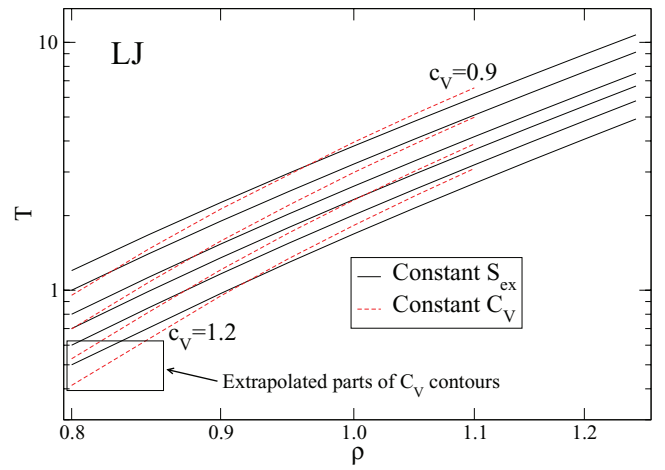
Figs. 4 and 5. It cannot be otherwise, but there is more information here compared to those figures. For example, the adiabats are closer to the straight lines (in the double-log representation) expected for IPL systems, while the C_V-contours have more non-trivial shapes. Furthermore a small variation of C_V along an adiabat could hide a relatively large difference in slope between C_V-contours and adiabats (since C_V is typically a relatively slowly varying function).

IV. FLUCTUATION FORMULA FOR GENERATING CONTOURS OF C_V

Apart from investigating the variation of C_V along an adiabat, it is of interest to identify the contours of C_V; the non-constancy of C_V along an adiabat is equivalent to the statement that the C_V contours do not coincide with the adiabats, although we can expect them to be close for Roskilde liquids.
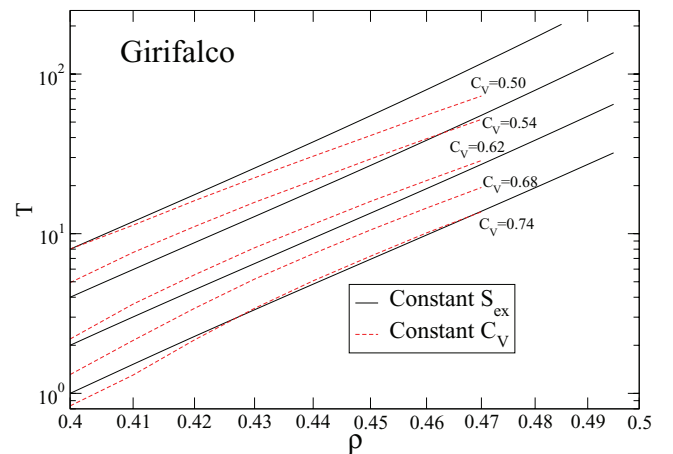

FIG. 7. Comparison of adiabats with C_V-contours for the Girifalco system. The adiabats were calculated using the definition of γ and small changes in ρ, while C_V-contours were determined from a series of simulations on different isochores and interpolating the C_V data as a function of T.

In practice, we identify C_V contours using the interpolation procedure described above, but it is potentially useful from a theoretical point of view to have a fluctuation formula for the slope of these curves. This we derive in this section.

Since the variation of C_V along an adiabat (Eq. (22)) involves the difference between two triple correlations $\langle(\Delta U)^2 \Delta(W - \gamma U)\rangle$ (which vanishes for perfect correlation); it is tempting to speculate that the ratio

$$\frac{\langle(\Delta U)^2 \Delta W\rangle}{\langle(\Delta U)^3\rangle}, \tag{42}$$

which equals γ for perfect correlation, gives the slope of curves of constant C_V. But it is not so simple. The total derivative of C_V with respect to $\ln \rho$ along an arbitrary slope g in the $(\ln \rho, \ln T)$ plane is

$$\left(\frac{\partial C_V}{\partial \ln \rho}\right)_{[g]} = \left(\frac{\partial C_V}{\partial \ln \rho}\right)_T + g\left(\frac{\partial C_V}{\partial \ln T}\right)_\rho. \tag{43}$$

We need to calculate the partial derivatives with respect to T and ρ. From Appendix D:

$$\left(\frac{\partial C_V}{\partial \ln T}\right)_\rho = -2\beta^2 \langle(\Delta U)^2\rangle - \beta^3 \frac{\partial\langle U^2\rangle}{\partial \beta} - 2\beta^3 \langle U\rangle\langle(\Delta U)^2\rangle. \tag{44}$$

From Eqs. (11) and (B8) we have

$$\frac{\partial\langle U^2\rangle}{\partial \beta} = -\langle \Delta U \Delta(U^2)\rangle \tag{45}$$

$$= -\langle \Delta U(2\langle U\rangle \Delta U + (\Delta U)^2 - \langle(\Delta U)^2\rangle)\rangle \tag{46}$$

$$= -2\langle U\rangle\langle(\Delta U)^2\rangle - \langle(\Delta U)^3\rangle. \tag{47}$$

Inserting this into Eq. (44) gives

$$\left(\frac{\partial C_V}{\partial \ln T}\right)_\rho = -2\beta^2 \langle(\Delta U)^2\rangle + \beta^3 \langle(\Delta U)^3\rangle. \tag{48}$$

It might seem surprising that the third moment appears, since one expects the limit of large N that the distribution converges to a Gaussian, in accordance with the central limit theorem. A closer look at the proof of that theorem shows that when considering the summed variable (here the total potential energy), all the so-called cumulants are proportional to N, and both the second and third moments are equal to the corresponding cumulants, and therefore proportional to N. It is when one considers the average instead of the sum (potential energy per particle instead of total potential energy) that one finds the third moment and cumulant vanishing faster than the second ($1/N^2$ as opposed to $1/N$) in the limit of large N.

The density derivative of C_V,

$$\left(\frac{\partial C_V}{\partial \ln \rho}\right)_T = \beta^2\left(\frac{\partial\langle U^2\rangle}{\partial \ln \rho}\right)_T - \beta^2 2\langle U\rangle\left(\frac{\partial\langle U\rangle}{\partial \ln \rho}\right)_T, \tag{49}$$

is evaluated in Appendix D with the result

$$\left(\frac{\partial C_V}{\partial \ln \rho}\right)_T = -\beta^3\langle\Delta W(\Delta U)^2\rangle + 2\beta^2\langle\Delta U \Delta W\rangle. \tag{50}$$

The derivative of C_V along an arbitrary slope g is then

$$\left(\frac{dC_V}{d\ln \rho}\right)_{[g]} = C_V\left(\frac{\beta\langle(\Delta U)^3\rangle g - \beta\langle(\Delta U)^2\Delta W\rangle}{\langle(\Delta U)^2\rangle} + 2(\gamma - g)\right). \tag{51}$$

Note that with $g = \gamma$ we recover Eq. (22). When the correlation is not perfect we can set this expression to zero and solve for the slope g which gives curves of constant C_V, now calling it $\gamma_{C_V} \equiv (\partial \ln T/\partial \ln \rho)_{C_V}$:

$$\gamma_{C_V}\left(\frac{\beta\langle(\Delta U)^3\rangle}{\langle(\Delta U)^2\rangle} - 2\right) = \frac{\beta\langle(\Delta U)^2\Delta W\rangle}{\langle(\Delta U)^2\rangle} - 2\gamma \tag{52}$$

or

$$\gamma_{C_V} = \frac{\langle(\Delta U)^2\Delta W\rangle - 2T\gamma\langle(\Delta U)^2\rangle}{\langle(\Delta U)^3\rangle - 2T\langle(\Delta U)^2\rangle}. \tag{53}$$

Again we check the case of perfect correlation where we can replace ΔW by $\gamma \Delta U$ and see that we get γ as we should. We can also write this as γ plus a correction term:

$$\gamma_{C_V} = \gamma + \frac{\langle(\Delta U)^2\epsilon\rangle}{\langle(\Delta U)^3\rangle - 2T\langle(\Delta U)^2\rangle}. \tag{54}$$

Figure 8 shows the fluctuation-determined slope γ_{C_V} of a C_V contour in the $(\ln \rho, \ln T)$-plane along the $C_V = 1.0$ contour of the LJ system. We present the C_V-contour here to be able to check the validity of the exponent: The (fixed) exponent determined by a fit of the contour to a power law is also indicated for comparison. A clear trend is observed with γ_{C_V} higher than γ, and like the latter decreasing towards 4 as the density increases. There is some scatter due to the difficulty in determining third moments (compare the data for γ which are based on second moments), so this would not be a practical method for determining the contours. On the other hand, if we are interested in knowing roughly how big the difference in slope between an adiabat and a C_V-contour is, we do not need to simulate a C_V-contour–we can simu-
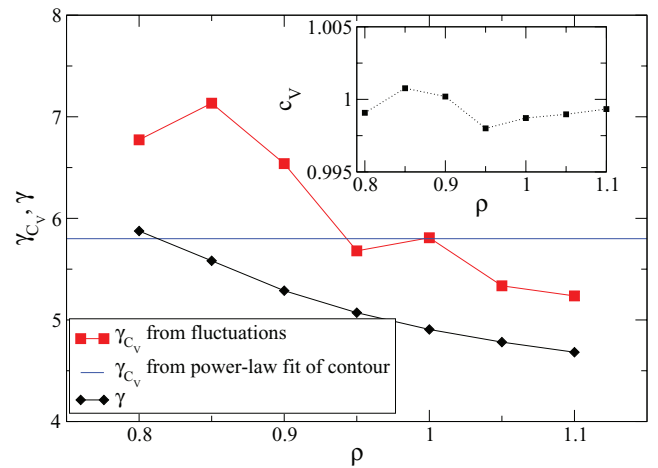

FIG. 8. Plot of $\gamma_{C_V} = (\partial \ln T/\partial \ln \rho)_{C_V}$ estimated from fluctuations, along the $C_V = 1.0$ contour for the LJ system. The contour was determined by interpolation. The horizontal line indicates the slope found by fitting the contour to a power-law form for comparison. The decrease of γ_{C_V} towards large densities is expected, just as with γ (also shown) since at high densities we expect both to converge to one third of the repulsive exponent, i.e., 4. The inset shows C_V versus ρ along the contour as a check that the contour was correctly determined.
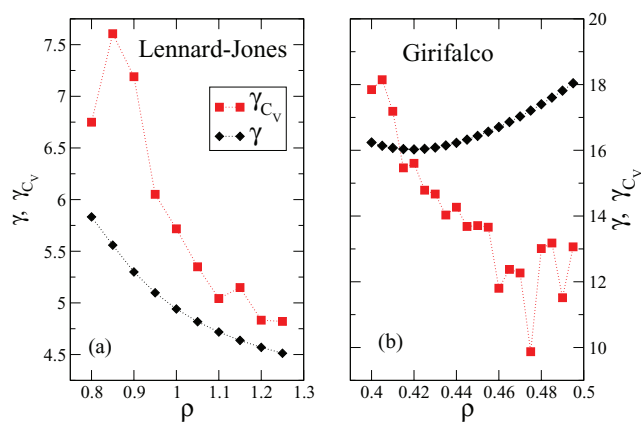
FIG. 9. Plot of $\gamma_{C_V} = (\partial \ln T / \partial \ln \rho)_{C_V}$ estimated from fluctuations, along (a) the adiabat including $\rho = 0.8$, $T = 0.8$ for the LJ system and (b) the adiabat including $\rho = 0.4$, $T = 4.0$ for the Girifalco system, as functions of ρ, compared to γ.

late a few state points, perhaps on an isochore, and estimate the γ_{C_V} from fluctuations. The scatter is not a big problem if we are not using γ_{C_V} to determine where to simulate next. Figure 9 compares γ_{C_V} with γ for both LJ and Girifalco system along an adiabat, and the trends are very clear: the C_V-contours have definitely larger slope for the LJ system, closer to 6 than 5 (they must converge to 4 at high density). For the Girifalco system the differences are quite dramatic, more so than the direct comparison of the contours in Fig. 7 (where a logarithmic temperature scale was used). It is worth noting that all the data here correspond to state points with $R > 0.985$, i.e., very strong U, W correlation, and that nothing special happens when the exponents are equal (e.g., $\rho \sim 0.42$ in Fig. 9(b)) (in any system one can define phase-space curves along which $\gamma - \gamma_{C_V} = 0$; it would be significant only if a two-dimensional region of equality existed).

V. DISCUSSION

A. Roskilde liquids are more than, and more interesting than, IPL liquids

IPL liquids are perfectly correlating and have perfect isomorphs—straight lines in the $(\ln \rho - \ln T)$ plane with slope given by one third of the IPL exponent. In this case the phase diagram is completely degenerate—the isomorphs are contours of excess entropy, C_V and all structural and dynamical properties (when expressed in reduced units). Liquids which have strong, but not perfect U, W correlation are much more interesting: we can still identify excellent isomorphs via Eq. (5), as adiabats, but these are no longer constrained to be power laws; the effective exponent can vary along an isomorph/adiabat and can exhibit non-trivial density dependence.[42] Moreover, C_V contours deviate now from the isomorphs/adiabats in a manner connected to the density dependence of γ.

It is interesting to compare the insight obtained from statistical mechanical versus thermodynamic considerations. Using statistical mechanics—the arguments leading to Eq. (38)—we have shown that $(\partial \gamma / \partial T)_\rho$ vanishes when cor-

relation is perfect, and this occurs only for (extended) IPL systems (see Eq. (30)). We have also argued that in liquids with strong but not perfect U, W correlations the temperature derivative is relatively small, therefore as a first approximation it can be ignored, leaving the density dependence of γ as a new characteristic for a Roskilde liquid. On the other hand the purely thermodynamic arguments presented in Ref. 32 constrain only $(\partial \gamma / \partial T)_\rho$ to be zero, leaving γ free to depend on density, which allows for the richer set of behaviors just mentioned. The thermodynamic argument leads more directly (and elegantly) to the empirical truth—that in practice γ's temperature dependence is small compared to its density dependence—while the statistical mechanical arguments fill in the details of why this is the case.

B. Is isomorph theory the zeroth term in a systematic expansion?

The isomorph theory was characterized in the introduction as a "zero-order" theory, analogous to the ideal gas. For the latter there exists a systematic expansion (the virial series, with the small parameter being density times molecular volume) for obtaining the equation of state for interacting systems, or for obtaining transport properties (kinetic theory).[45,46] It is an open question whether a similar expansion exists where perfect isomorphs correspond to the zeroth term. If so, one could quantify the errors made in using the isomorph theory. A natural starting point might be thermodynamic perturbation theory using an IPL reference system, but here caution should be advised, because this would ignore that fact γ varies along an isomorph and in any case we do not have exact or near exact analytical solution for the thermodynamics and structure of the IPL system. Furthermore, traditional thermodynamic perturbation theory is primarily concerned with thermodynamics (equation of state), less so with structure, and not much at all with dynamics; isomorph theory makes predictions primarily for structure, dynamics, and some thermodynamic quantities but in general not the equation of state as such (though see Refs. 22 and 47). In particular, the use of variational perturbation theory to estimate the IPL exponent at a given state point through an optimal perturbation estimate of the free energy typically finds an exponent larger than γ.[48]

C. Status of $n^{(2)}$ and relation between different γ derivatives

The claim (38) needs to be thoroughly investigated by simulation for a wider range of systems as does the validity of Eq. (31) as an estimate of γ. While we have argued these for high temperatures and densities, their validity could turn out to depend on how strong U, W-correlation a liquid has, though it seems that $R > 0.9$ is not necessarily required, that is, they apply more generally than strong U, W correlation. One could imagine that it would be useful to derive a fluctuation formula for $(\partial \gamma / \partial \rho)_S$. We have indeed derived such a formula, see Appendix E, but it is not particularly simple, and we have not been able to use it to make a more rigorous theoretical connection with $(\partial \gamma / \partial T)_\rho$—even the sign

is far from obvious due to near cancellation of the various terms. Its usefulness in simulations is also expected to be limited since it involves fluctuations of the so-called hyper-virial (the quantity used to determine the bulk modulus from fluctuations[49]) which is not typically available in a MD simulation. On the other hand, from the other results presented here, one can use the quantity $\langle (\Delta U)^2 \epsilon \rangle$ or the formula for γ_{C_V} to determine the sign of $(\partial \gamma / \partial \rho)_S$ from a simulation of a single state point.

D. Adiabats versus C_V contours in non-Roskilde-simple liquids

It is interesting to consider a non-simple liquid, where there is no reason to expect that C_V-contours at all coincide with adiabats (i.e., there are not good isomorphs). We have done so for two liquids without actually determining the C_V-contours; instead we just calculated the exponent γ_{C_V} from the fluctuations. As mentioned above this is accurate enough to give an idea of the trends, in particular which way the C_V-contours are oriented with respect to the adiabats. The first example is the Dzugutov fluid.[37] Figure 10 shows γ_{C_V} and γ for this system along an adiabat. In the range shown R takes values from ~ 0.56 to ~ 0.84. As the figure shows γ_{C_V} is substantially smaller than γ. We can note also that this is consistent with the positive slope $d\gamma/d\rho$, and suggests the arguments leading to Eq. (38) do not necessarily require strong W, U correlation. The Lennard-Jones-Gaussian system[15] behaves similarly (data not shown). A very different example is the Gaussian core potential,[14] which lacks a hard core (thus particles can overlap/penetrate each other) for which data is also shown in Fig. 10. In this case there is almost no W, U correlation; $0.16 > R > 0.06$, and in fact γ_{C_V} and γ even have opposite sign (although both are close to zero). Moreover, this system clearly violates Eq. (38), since γ decreases with density on the adiabat shown, which should correspond to the case $\gamma_{C_V} > \gamma$ (as in the LJ case); this is not surprising since it does not have a hard core.
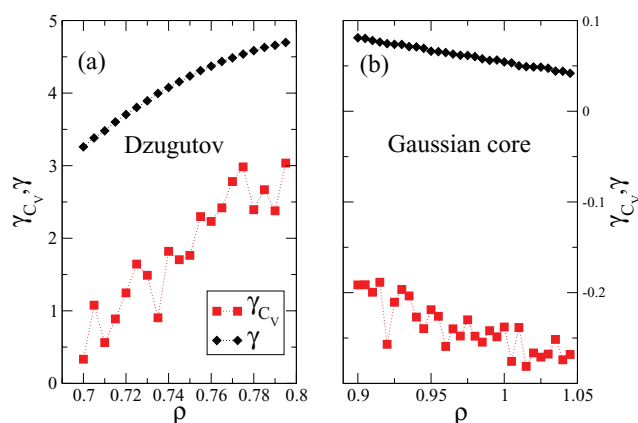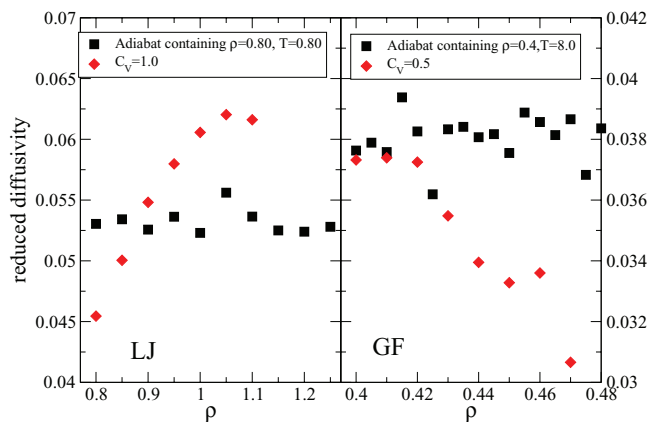

FIG. 11. Diffusivity in reduced units versus density along an adiabat and along a C_V-contour for the LJ and GF systems. It is more or less invariant on the adiabats but not on the C_V-contours.

E. Relevance of adiabats versus C_V contours

In our simulation studies of isomorphs, the procedure has always been to use Eq. (5) to generate adiabats (straightforward, since an accurate estimate of γ is readily computed from the W, U fluctuations) and then examine to what extent the other isomorph-invariant quantities are actually invariant along these curves. One could also generate C_V contours and check for invariance along them. While it is not obvious that adiabats are more fundamental, Rosenfeld proposed that transport properties are in fact governed by the excess entropy.[50] Given the not insignificant difference between adiabats and C_V-contours it is worth checking explicitly whether measures of dynamics are more invariant along one versus the other. This is done in Fig. 11 for the reduced diffusivity $\tilde{D} \equiv \left(\rho^{1/3} \sqrt{m/T} \right) D$. It is clear that by the this measure, the dynamics are more invariant along adiabats than along C_V-contours, consistent with Rosenfeld's theory. We note also that the adiabats seem to be simpler than the C_V-contours in that the exponent γ varies less than the exponent γ_{C_V}. This is true for the all the systems presented here including simple and non-simple ones. This implies γ is more practical as a liquid characteristic than γ_{C_V} and suggests that adiabats provide a more useful, and fundamental basis for describing the phase diagram than C_V-contours. In fact a (ρ, S) phase diagram would be consistent with the traditional starting point of statistical mechanics—a function $U(S, V)$ expressing the dependence of internal energy on entropy and volume (though typically the total entropy, not S, is considered).

VI. CONCLUSION

We have derived several exact results relating to Roskilde-simple liquids (previously termed strongly correlating liquids) in the form of fluctuation formulas for various thermodynamic derivatives. These include the derivative (with respect to $\ln \rho$) of an arbitrary NVT averaged dynamical variable along a configurational adiabat, Eq. (17), the derivative of C_V along an adiabat, Eq. (22), the temperature derivative of γ itself on an isochore, Eq. (27), and the slope of contours of C_V in the $(\ln \rho, \ln T)$ plane, Eq. (53). In addition to

FIG. 10. Plot of $\gamma_{C_V} = (\partial \ln T / \partial \ln \rho)_{C_V}$ estimated from fluctuations, for (a) the Dzugutov system along the adiabat including $\rho = 0.70$, $T = 0.70$ and (b) the Gaussian core system along the adiabat including at $\rho = 0.90$, $T = 0.75$, as functions of ρ, compared to γ.

the exact formulas we have argued that when $d\gamma/d\rho$ is negative (positive) one expects that $(\partial C_V/\partial\rho)_S$ is positive (negative) and that the slopes of C_V-contours are greater (less) than those of adiabats. This we have tested with two model Roskilde-simple liquids, the Lennard-Jones fluid with $d\gamma/d\rho < 0$ and the Girifalco potential which has $d\gamma/d\rho < 0$ at low density but switches to $d\gamma/d\rho > 0$ at high density. From this argument emerged a claim, Eq. (38) equating the sign of the temperature derivative of γ to the density derivative along an adiabat for a wide class of liquids (wider than Roskilde-simple liquids). Finally, we note that the data presented here provide support for the use of the $n^{(2)}$ exponent, determined purely by the pair potential, as a quick and convenient way to estimate γ and its density dependence.

APPENDIX A: DERIVATION OF EQ. (13)

As in Appendix A of Ref. 18, we use a discrete-state notation for convenience, such that A_i is the value of observable A in microstate i and the (configurational) partition function is $Z = \sum_i \exp(-\beta U_i)$. We have

$$\left(\frac{\partial\langle A\rangle}{\partial\ln\rho}\right)_T$$

$$= \frac{1}{Z}\frac{\partial\sum_i A_i\exp(-\beta U_i)}{\partial\ln\rho}$$

$$- \frac{1}{Z^2}\sum_i A_i\exp(-\beta U_i)\frac{\partial\sum_j\exp(-\beta U_j)}{\partial\ln\rho} \quad \text{(A1)}$$

$$= \frac{1}{Z}\sum_i\left(\frac{\partial A_i}{\partial\ln\rho}\exp(-\beta U_i) + A_i\exp(-\beta U_i)(-\beta)\frac{\partial U_i}{\partial\ln\rho}\right)$$

$$- \frac{\sum_i A_i\exp(-\beta U_i)}{Z^2}\sum_j\exp(-\beta U_j)(-\beta)\frac{\partial U_i}{\partial\ln\rho} \quad \text{(A2)}$$

$$= \left\langle\frac{\partial A}{\partial\ln\rho}\right\rangle - \beta(\langle AW\rangle - \langle A\rangle\langle W\rangle) \quad \text{(A3)}$$

$$= \left\langle\frac{\partial A}{\partial\ln\rho}\right\rangle - \beta\langle\Delta A\Delta W\rangle. \quad \text{(A4)}$$

In the second last step the definition of the virial for a micro-configuration, $W_i \equiv (\partial U_i/\partial\ln\rho)$, was used; the density derivative is understood to mean that the reduced coordinates are held fixed while the volume is changed.

APPENDIX B: DERIVATION OF EQ. (22)

Here we give the details of the derivation of the expression for the derivative of C_V at constant S. Writing the variance of U as $\langle(\Delta U)^2\rangle = \langle U^2\rangle - \langle U\rangle^2$ allows us to use Eq. (17) to take the derivative of $\langle U^2\rangle$ and Eq. (18) to

differentiate $\langle U\rangle$:

$$\left(\frac{\partial\langle(\Delta U)^2\rangle}{\partial\ln\rho}\right)_S$$

$$= \left\langle\frac{\partial U^2}{\partial\ln\rho}\right\rangle - \beta\langle\Delta(U^2)\Delta(W-\gamma U)\rangle - 2\langle U\rangle\langle W\rangle \quad \text{(B1)}$$

$$= \langle 2UW\rangle - \beta\langle\Delta(U^2)\Delta(W-\gamma U)\rangle - 2\langle U\rangle\langle W\rangle \quad \text{(B2)}$$

$$= 2\langle\Delta U\Delta W\rangle - \beta\langle\Delta(U^2)\Delta(W-\gamma U)\rangle \quad \text{(B3)}$$

$$= 2\gamma\langle(\Delta U)^2\rangle - \beta\langle\Delta(U^2)\Delta(W-\gamma U)\rangle, \quad \text{(B4)}$$

where we have used Eq. (3) to write the covariance $\langle\Delta U\Delta W\rangle$ in terms of the variance of U. Inserting this result into Eq. (21) gives the relatively simple formula

$$\left(\frac{\partial C_V}{\partial\ln\rho}\right)_S = -\beta^3\langle\Delta(U^2)\Delta(W-\gamma U)\rangle = -\beta^3\langle\Delta(U^2)\epsilon\rangle. \quad \text{(B5)}$$

We make one more change by writing $U = \langle U\rangle + \Delta U$, so that

$$\Delta(U^2) = U^2 - \langle U^2\rangle \quad \text{(B6)}$$

$$= \langle U\rangle^2 + 2\langle U\rangle\Delta U + (\Delta U)^2 - (\langle U\rangle^2 + \langle(\Delta U)^2\rangle) \quad \text{(B7)}$$

$$= 2\langle U\rangle\Delta U + (\Delta U)^2 - \langle(\Delta U)^2\rangle. \quad \text{(B8)}$$

When this is correlated with $\epsilon = \Delta W - \gamma\Delta U$, the first term vanishes because of Eq. (10) and the last term vanishes because $\langle\epsilon\rangle = 0$. Thus $\langle\Delta(U^2)\epsilon\rangle = \langle(\Delta U)^2\epsilon\rangle$ and we arrive at Eq. (22).

APPENDIX C: GENERATING CONFIGURATIONAL ADIABATS

Equation (5) indicates a general procedure for generating adiabats: (1) evaluate γ from the fluctuations at the current state point; (2) choose a small change in density, say of order 1% or less; (3) use Eq. (5) to determine the corresponding change in temperature:

$$\rho_{n+1} = \rho_n + \delta\rho, \quad \text{(C1)}$$

$$T_{n+1} = T_n(\rho_{n+1}/\rho_n)^{\gamma_n}. \quad \text{(C2)}$$

We have used this method for the Girifalco system with $\delta\rho = 0.005$ for values of ρ between 0.4 and 0.5. For generalized Lennard-Jones systems there is now an analytic expression for the ρ-dependence of γ which allows large changes in ρ, the so-called "long jump method":[32, 33]

$$\rho_{n+1} = \rho_n + \delta\rho, \quad \text{(C3)}$$

$$T_{n+1} = T_n h(\alpha_n, \rho_{n+1})/h(\alpha_n, \rho_n), \quad \text{(C4)}$$

where the energy/temperature scaling function $h(\alpha, \rho)$ is defined by (see Refs. 32 and 33; the normalization is such that $h(\alpha, 1) = 1$).

$$h(\alpha, \rho) = \alpha\rho^4 + (1 - \alpha)\rho^2. \tag{C5}$$

Here α is a parameter which according to the theory of isomorphs—i.e., assuming perfect isomorphs for LJ systems—is a constant. More generally one may expect that it is fixed for a given isomorph, but can vary weakly among isomorphs, analogous to $\Lambda(S)$ in Eq. (31). In fact, since $\gamma = d\ln(h)/d\ln(\rho),^{32}$ there is a close connection between $h(\rho)$ and $n^{(2)}$; by identifying Eq. (31) with the logarithmic derivative of $h(\rho)$ we find that the latter can be expressed generally in terms of the curvature of the pair potential:

$$h(\rho) = \rho^{-2/3}v''(\Lambda(S)\rho^{-1/3}), \tag{C6}$$

making it clear how to include dependence on S in $h(\rho)$. This connection will be discussed in more detail elsewhere.[42] At a given density α can be evaluated via

$$\alpha = (\gamma - 2)/(4\rho^2 - 2 - \gamma\rho^2 + \gamma) \tag{C7}$$

(at $\rho = 1$ this becomes simply $\gamma/2 - 1$).

Since the theory is not exact, and α determined this way will also vary weakly along the isomorph, in order to get the best determination of the adiabats we re-evaluate α at each state point. It therefore also has an index n. We observe a systematic variation in α of at most 0.5% for a given adiabat, and a few percent variation between adiabats. We have used the long-jump formula for the LJ system with $\delta\rho = 0.05$ for values of ρ between 0.8 and 1.4. We noticed more noise in the data for the Girifalco system, but have not checked whether this is due to not having a long-jump formula or to differences in effective sampling rate (because of different relaxation times) giving different statistical errors.

APPENDIX D: DERIVATION OF C_V EXPONENT

The temperature derivative of C_V, Eq. (44), is obtained as follows:

$$\left(\frac{\partial C_V}{\partial \ln T}\right)_\rho$$

$$= -\frac{\partial}{\partial \ln \beta}(\beta^2\langle(\Delta U)^2\rangle) = -\beta\frac{\partial}{\partial \beta}(\beta^2\langle(\Delta U)^2\rangle) \tag{D1}$$

$$= -2\beta^2\langle(\Delta U)^2\rangle - \beta^3\frac{\partial}{\partial \beta}(\langle U^2\rangle - \langle U\rangle^2) \tag{D2}$$

$$= -2\beta^2\langle(\Delta U)^2\rangle - \beta^3\frac{\partial\langle U^2\rangle}{\partial \beta} + 2\beta^2\langle U\rangle\beta\frac{\partial\langle U\rangle}{\partial \beta} \tag{D3}$$

$$= -2\beta^2\langle(\Delta U)^2\rangle - \beta^3\frac{\partial\langle U^2\rangle}{\partial \beta} - 2\beta^2\langle U\rangle TC_V \tag{D4}$$

$$= -2\beta^2\langle(\Delta U)^2\rangle + \beta^3\langle(\Delta(U^2)\Delta U\rangle - 2\beta^3\langle U\rangle\langle(\Delta U)^2\rangle. \tag{D5}$$

In the last line Eq. (11) was used. We can simplify by using Eq. (B8):

$$\left(\frac{\partial C_V}{\partial \ln T}\right)_\rho = -2\beta^2\langle(\Delta U)^2\rangle + \beta^3(2\langle U\rangle\langle(\Delta U)^2\rangle + \langle(\Delta U)^3\rangle)$$

$$- 2\beta^3\langle U\rangle\langle(\Delta U)^2\rangle \tag{D6}$$

$$= -2\beta^2\langle(\Delta U)^2\rangle + \beta^3\langle(\Delta U)^3\rangle. \tag{D7}$$

For the density derivative of C_V, we have likewise,

$$\left(\frac{\partial C_V}{\partial \ln \rho}\right)_T = \beta^2\left(\frac{\partial\langle U^2\rangle}{\partial \ln \rho}\right)_T - \beta^2 2\langle U\rangle\left(\frac{\partial\langle U\rangle}{\partial \ln \rho}\right)_T. \tag{D8}$$

Starting with the second term, using Eq. (13),

$$\left(\frac{\partial\langle U\rangle}{\partial \ln \rho}\right)_T = -\beta\langle\Delta W\Delta U\rangle + \langle W\rangle \tag{D9}$$

while the first gives, also using Eqs. (13) and (B8),

$$\left(\frac{\partial\langle U^2\rangle}{\partial \ln \rho}\right)_T$$

$$= -\beta\langle\Delta W\Delta(U^2)\rangle + \langle 2UW\rangle \tag{D10}$$

$$= -2\beta\langle U\rangle\langle\Delta W\Delta U\rangle - \beta\langle\Delta W(\Delta U)^2\rangle + 2\langle UW\rangle. \tag{D11}$$

Combining the two terms then gives

$$\left(\frac{\partial C_V}{\partial \ln \rho}\right)_T = -\beta^3 2\langle U\rangle\langle\Delta U\Delta W\rangle - \beta^3\langle\Delta W(\Delta U)^2\rangle$$

$$+ 2\beta^2\langle UW\rangle + 2\langle U\rangle\beta^3\langle\Delta W\Delta U\rangle - 2\langle U\rangle\beta^2\langle W\rangle \tag{D12}$$

$$= -\beta^3\langle\Delta W(\Delta U)^2\rangle + 2\beta^2\langle\Delta U\Delta W\rangle \tag{D13}$$

which is Eq. (50). Now we can assemble the derivative of C_V along an arbitrary slope g (Eq. (43)),

$$\left(\frac{dC_V}{d\ln \rho}\right)_{[g]} = -\beta^3\langle\Delta W(\Delta U)^2\rangle + 2\beta^2\langle\Delta U\Delta W\rangle$$

$$+ g(-2\beta^2\langle(\Delta U)^2\rangle + \beta^3\langle(\Delta U)^3\rangle) \tag{D14}$$

$$= \beta^2\langle(\Delta U)^2\rangle(-\beta\langle\Delta W(\Delta U)^2\rangle/\langle(\Delta U)^2\rangle + 2\gamma$$

$$+ g(-2 + \beta\langle(\Delta U)^3\rangle/\langle(\Delta U)^2\rangle)) \tag{D15}$$

which can be rewritten as Eq. (51).

APPENDIX E: FLUCTUATION FORMULA FOR THE DERIVATIVE OF γ

We include here, omitting the derivation, the fluctuation formula for the derivative of γ with respect to $\ln \rho$ at constant

S. The quantity $X \equiv dW/d \ln \rho$ is the hypervirial, which appears in fluctuation expressions for the bulk modulus.[49]

$$\left(\frac{\partial \gamma}{\partial \ln \rho} \right)_S = \frac{1}{\langle (\Delta U)^2 \rangle} (\langle (\Delta W)^2 \rangle + \langle \Delta U \, \Delta X \rangle$$
$$- 2\gamma^2 \langle (\Delta U)^2 \rangle - \beta \langle \Delta U \epsilon^2 \rangle). \quad \text{(E1)}$$

For IPL systems (and perfect correlating systems in general) we have $\Delta X = \gamma \Delta W = \gamma^2 \Delta U$ and $\epsilon \equiv 0$, so that the derivative is zero.

[1] I. Z. Fisher, *Statistical Theory of Liquids* (University of Chicago, Chicago, 1964).

[2] S. A. Rice and P. Gray, *The Statistical Mechanics of Simple Liquids* (Interscience, New York, 1965).

[3] H. N. V. Temperley, J. S. Rowlinson, and G. S. Rushbrooke, *Physics of Simple Liquids* (Wiley, 1968).

[4] N. K. Ailawadi, Phys. Rep. **57**, 241 (1980).

[5] J. S. Rowlinson and B. Widom, *Molecular Theory of Capillarity* (Clarendon, Oxford, 1982).

[6] C. G. Gray and K. E. Gubbins, *Theory of Molecular Fluids* (Oxford University Press, 1984).

[7] D. Chandler, *Introduction to Modern Statistical Mechanics* (Oxford University Press, 1987).

[8] J. L. Barrat and J. P. Hansen, *Basic Concepts for Simple and Complex Liquids* (Cambridge University Press, 2003).

[9] P. G. Debenedetti, AIChE J. **51**, 2391 (2005).

[10] J. P. Hansen and I. R. McDonald, *Theory of Simple Liquids*, 3rd ed. (Academic Press, New York, 1986).

[11] J. F. Douglas, J. Dudowicz, and K. F. Freed, J. Chem. Phys. **127**, 224901 (2007).

[12] B. Kirchner, Phys. Rep. **440**, 1 (2007).

[13] B. Bagchi and C. Chakravarty, J. Chem. Sci. **122**, 459 (2010).

[14] F. H. Stillinger, J. Chem. Phys. **65**, 3968 (1976).

[15] M. Engel and H.-R. Trebin, Phys. Rev. Lett. **98**, 225505 (2007).

[16] V. Van Hoang and T. Odagaki, Physica B **403**, 3910 (2008).

[17] T. S. Ingebrigtsen, T. B. Schrøder, and J. C. Dyre, Phys. Rev. X **2**, 011011 (2012).

[18] N. P. Bailey, U. R. Pedersen, N. Gnan, T. B. Schrøder, and J. C. Dyre, J. Chem. Phys. **129**, 184507 (2008).

[19] N. P. Bailey, U. R. Pedersen, N. Gnan, T. B. Schrøder, and J. C. Dyre, J. Chem. Phys. **129**, 184508 (2008).

[20] T. B. Schrøder, N. P. Bailey, U. R. Pedersen, N. Gnan, and J. C. Dyre, J. Chem. Phys. **131**, 234503 (2009).

[21] N. Gnan, T. B. Schrøder, U. R. Pedersen, N. P. Bailey, and J. C. Dyre, J. Chem. Phys. **131**, 234504 (2009).

[22] T. B. Schrøder, N. Gnan, U. R. Pedersen, N. P. Bailey, and J. C. Dyre, J. Chem. Phys. **134**, 164505 (2011).

[23] J. K. Johnson, J. A. Zollweg, and K. E. Gubbins, Mol. Phys. **78**, 591 (1993).

[24] E. A. Mastny and J. J. de Pablo, J. Chem. Phys. **127**, 104504 (2007).

[25] V. V. Brazhkin, Y. D. Fomin, A. G. Lyapin, V. N. Ryzhov, and K. Trachenko, JETP Lett. **95**, 164 (2012).

[26] V. V. Brazhkin, Y. D. Fomin, A. G. Lyapin, V. N. Ryzhov, and K. Trachenko, Phys. Rev. E **85**, 031203 (2012).

[27] V. V. Brazhkin, Y. D. Fomin, A. G. Lyapin, V. N. Ryzhov, E. N. Tsiok, and K. Trachenko, Phys. Rev. Lett. **111**, 145901 (2013).

[28] U. R. Pedersen, N. Gnan, N. P. Bailey, T. B. Schrøder, and J. C. Dyre, J. Non-Cryst. Solids **357**, 320 (2011).

[29] A. A. Veldhorst, L. Bøhling, J. C. Dyre, and T. B. Schrøder, Eur. Phys. J. B **85**, 21 (2012).

[30] T. S. Ingebrigtsen, T. B. Schrøder, and J. C. Dyre, J. Phys. Chem. B **116**, 1018 (2012).

[31] N. Gnan, C. Maggi, T. B. Schrøder, and J. C. Dyre, Phys. Rev. Lett. **104**, 125902 (2010).

[32] T. S. Ingebrigtsen, L. Bøhling, T. B. Schrøder, and J. C. Dyre, J. Chem. Phys. **136**, 061102 (2012).

[33] L. Bøhling, T. S. Ingebrigtsen, A. Grzybowski, M. Paluch, J. C. Dyre, and T. B. Schrøder, New J. Phys. **14**, 113035 (2012).

[34] D. Gundermann, U. R. Pedersen, T. Hecksher, N. P. Bailey, B. Jakobsen, T. Christensen, N. B. Olsen, T. B. Schrøder, D. Fragiadakis, R. Casalini *et al.*, Nat. Phys. **7**, 816 (2011).

[35] U. R. Pedersen, N. P. Bailey, T. B. Schrøder, and J. C. Dyre, Phys. Rev. Lett. **100**, 015701 (2008).

[36] A. Malins, J. Eggers, and C. P. Royall, "Investigating isomorphs with the topological cluster classification," preprint arXiv:1307.5516 (2013).

[37] M. Dzugutov, Phys. Rev. A **46**, R2984 (1992).

[38] L. A. Girifalco, J. Phys. Chem. **96**, 858 (1992).

[39] See http://rumd.org for the RUMD source code.

[40] H. Robbins and J. Van Ryzin, *Introduction to Statistics* (Science Research Associates, 1975).

[41] To "correlate with" means to multiply by and take an ensemble average.

[42] L. Bøhling, N. B. Bailey, T. B. Schrøder, and J. C. Dyre, "Estimating the density-scaling exponent of a liquid from its pair potential" (unpublished).

[43] Our method of determining Λ fails when $n^{(2)}$ is constant, but the value of r where one should evaluate $n^{(2)}$ is in principle well-defined.

[44] Y. Rosenfeld and P. Tarazona, Mol. Phys. **95**, 141 (1998).

[45] H. Smith and H. H. Jensen, *Transport Phenomena* (Oxford University Press, USA, 1989).

[46] S. G. Brush, *Kinetic Theory* (Pergamon Press, 1972), Vol. 3.

[47] J. C. Dyre, Phys. Rev. E **88**, 042139 (2013).

[48] N. P. Bailey, T. B. Schrøder, and J. C. Dyre, "Non-uniqueness of effective inverse power-law exponent for Lennard-Jones potential from variational perturbation theory" (unpublished).

[49] M. P. Allen and D. J. Tildesley, *Computer Simulation of Liquids* (Oxford University Press, 1987).

[50] Y. Rosenfeld, J. Phys.: Condens. Matter **11**, 5415 (1999).